SUPPLEMENTARY MATERIALS AND METHODS

Oligoprimers

All oligoprimers used for this study were designed using the Primer3 website (http://frodo.wi.mit.edu/primer3/) and are listed below in 5' --> 3' orientation by assay type. Sense oligoprimers are indicated by "Fw" and antisense by "Rv".

Chromatin Immunoprecipitation (ChIP)

Pro Fw	CTGGAACCTGCTCTCAAAGG
Pro Rv	AAAGGAGGTGGGGAGAGAC
SI_A Fw	AGCTGTGGGGCTCTACTTTG
SI_A Rv	TGAGCCATGCCTTTACATCA
SI_B Fw	TAGAGCCTGCTGCGTACCTC
SI_B Rv	CTGGCAGGCACTGAACACTT
Down_5kb Fw	GTGATGAAGGTGCCAGTTTCCTG
Down_5kb Rv	ACTCATCTCTCCTTTGGAGCTGG
Wnt3 Fw	CTCGCTGACATCCTCAAACC
Wnt3 Rv	TGAGGTTGGAAATGACTTTCG
OUT Fw	GCCAGCCTGAGCTATATGGA
OUT Rv	TGGACGCTGGGAACTAAATC

qRT-PCR

Pbx1 Fw	ACATGCTTTAAACTGCCACAGA
Pbx1 Rv	GTTGTCCAGTCGCATGAGC
Vimentin Fw	CGGAAAGTGGAATCCTTGCA
Vimentin Rv	CACATCGATCTGGACATGCTGT
TBP Fw	CTATCACTCCTGCCACACCA
TBP Rv	CAGTTGTCCGTGGCTCTCTT

The following RT-PCR oligoprimers were purchased from Qiagen (QuantiTect Primer Assays):

Snail1	QT00240940* Semi-quantitative RT-PCR
Smad4	QT00130585* Semi-quantitative RT-PCR
E-cadherin	QT00121163* Semi-quantitative RT-PCR

Reporter Assays

The SI-Pro construct used in luciferase assays contained the murine WT *Snail1* Promoter fragment (Pro; 951bp) and a *Snail1* second intron fragment (SI_A; 368 bp). These two fragments were amplified from C57/BL6 murine genomic DNA and cloned respectively into BglII/HindIII and KpnI restriction sites of the pGL4 (Promega) luciferase vector. The mutant construct (SI-mutPro) contains a 25 bp deletion designed to remove the two Pbx-binding sites present in the promoter (-557-531).

The following oligoprimers were used to generate the WT SI-Pro construct:

SI Fw	atgcggtaccAGCTGTGGGGCTCTACTTTG
SI Rv	atgcggtaccGTGTTCCTGGCAAGTGTGAA
Pro Fw	atgcagatctTGTGAACGTTCCAACACGAT
Pro Rv	atgcaagctt GACCTAGGTAGTCGGGGTCA

The following oligoprimers were used to generate the mutant SI-mutPro construct:

mutPro Fw	TCTAGGAAGTCATAGACACCCTCCCTCACAGCTGTCTCTCCCCACC
mutPro Rv	GGTGGGGAGAGACAGCTGTGAGGGAGGGTGTCTATGACTTCCTAGA

Antibodies

Primary Antibodies are listed below by assay type.

Western Blot (dilution 1:1000)

Pbx1a/b	Cell Signaling, 4342
Snail1/2	Abcam, ab85931 (discontinued)
E-cadherin	R&D Systems, AF748
Vimentin	Sigma, V2258
Smad4	Santa Cruz Biotechnology, sc-7966
Actin	Santa Cruz Biotechnology, sc-1616
Claudin3	Abcam, ab15102

Immunofluorescence (dilution 1:100)

ß-galactosidase	Abcam, ab9361
Vimentin	Sigma, V2258
Active caspase-3	Promega, G7481
Claudin3	Abcam, ab15102
E-cadherin	R&D Systems, AF748
Laminin	Sigma, L9393
Snail1/2	Abcam, ab85931 (discontinued)
Snail1	Cell Signaling, 3879
Smad4	Santa Cruz Biotechnology, sc-7966
Pbx1	Cell Signaling, 4342

Prep1/2	Santa Cruz Biotechnology, sc-6245
GFP	Aves Labs, GFP-1020
TUNEL	Sigma, 12156792910

Chromatin Immunoprecipitation (5 µg Ab used for each ChIP reaction)

Pbx1a/b	Cell Signaling, 4342
H3K27ac	Abcam, ab4729
H3K27me3	Millipore, 07-449
Rabbit IgG control	Cell Signaling, 2729

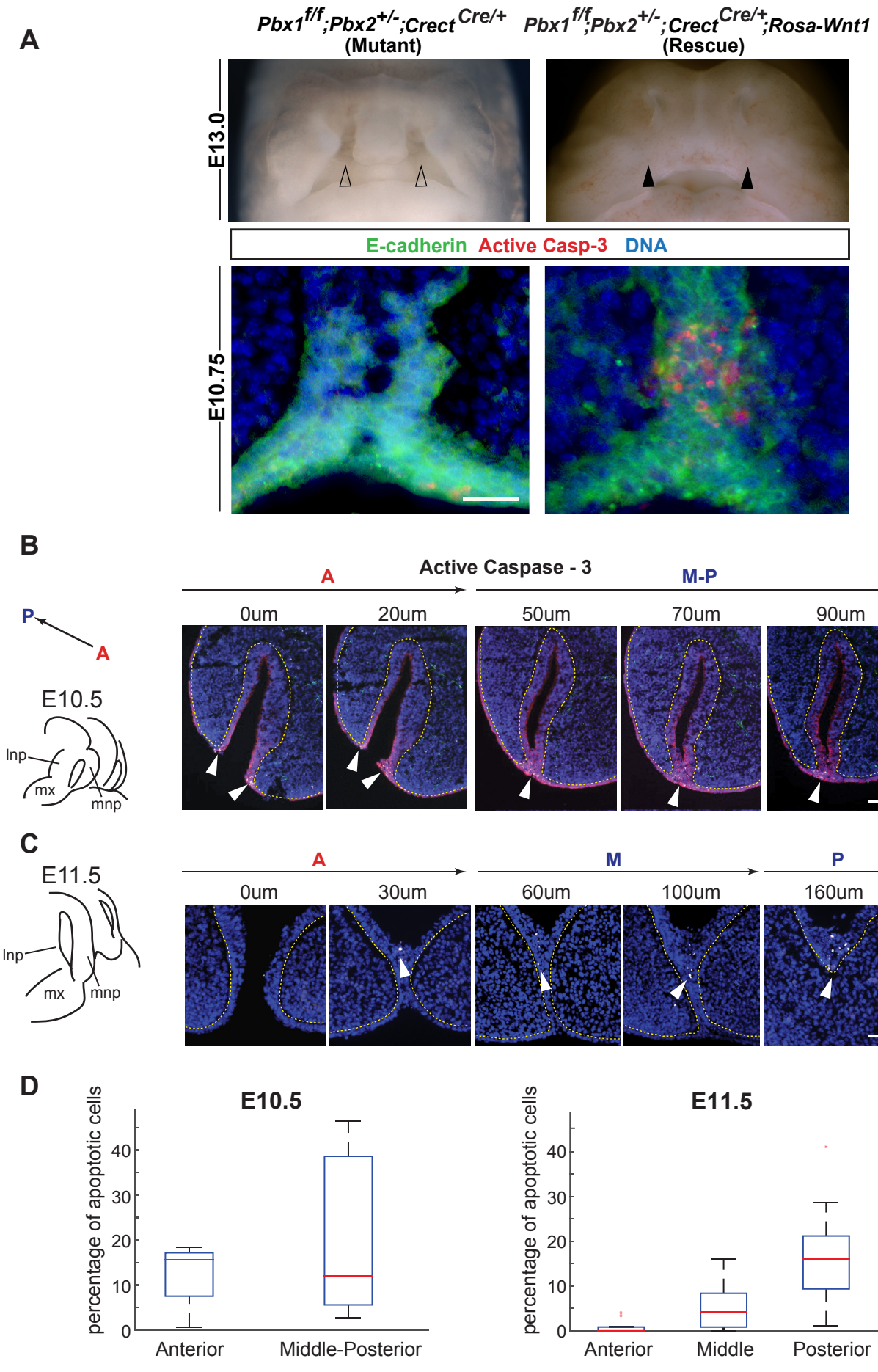

Figure S1. Rescue of orofacial clefting in *Pbx1/2* mutant embryos is accompanied by restored apoptosis, a dynamic and spatio-temporally regulated process at the lambdoidal junction. (A) Top panel: complete rescue of the CL phenotype in *Pbx1*$^{f/f}$*;Pbx2*$^{+/-}$*;Crect*$^{Cre/+}$ mutant embryos at E13.0 via ectopic expression of *Wnt1* in Crect-positive surface cephalic epithelial cells, as reported (Ferretti et al., 2011). Empty black arrowheads point to bilateral clefting of the upper lip; full black arrowheads indicate rescue of upper lip fusion. Bottom panel: triple immunofluorescence of E10.75 lambdoidal junction in *Pbx1/2* mutant and rescued embryo. Staining for epithelial E-cadherin (green), active caspase-3 (red) and DAPI (blue). While apoptosis at the λ is negligible or absent in *Pbx1*$^{f/f}$*;Pbx2*$^{+/-}$*;Crect*$^{Cre/+}$ mutant, as previously described (Ferretti et al., 2011), it is restored in *Pbx1*$^{f/f}$*;Pbx2*$^{+/-}$*;Crect*$^{Cre/+}$*;Rosa-Wnt1* rescued embryo. Scale bars; 20 μm. (B,C) Left: sketches of E10.5 (B) and E11.5 (C) embryonic midface structures. Medial and lateral nasal prominences (mnp and lnp) and maxillary prominence (mx) are defined. Arrow from A (anterior, red) to P (posterior, blue) indicates relative positions of sections representing anterior through middle (M) to posterior planes. Immunofluorescence for active caspase-3 (white signal; solid white arrowheads) in a series of coronal sections from E10.5 (B; A, M-P) and E11.5 (C; A,M,P) control λ junction. At both time-points, 0 μm is arbitrarily assigned to the section corresponding to the most exterior surface of the midface. At E10.5 progressively deeper sections are shown through the λ junction to the point wherein fusion of the prominences is almost complete (90 μm for E10.5). At E11.5 progressively deeper sections are shown that reach the level wherein fusion of the prominences is complete (160 μm for E11.5). Nuclei are labeled with DAPI (blue). Ectodermal epithelium at the λ junction is delimited by dashed lines and visualized by E-Cadherin staining (red) at E10.5. Scale bars: 50 μm. (D) Quantitation of apoptotic cells for each indicated domain of the λ junction was carried out by MATLAB on 20-30 sections from at least 3 embryos. The box-and-whisker plots depict percentage of apoptotic cells (Y axis) for each indicated domain (X axis) of E10.5 and E11.5 embryos. Blue boxes represent the middle 50% of the values of the sample range; red lines represent the value of the median; whiskers represent upper and lower limits of the sample. Red asterisks indicate outliers.

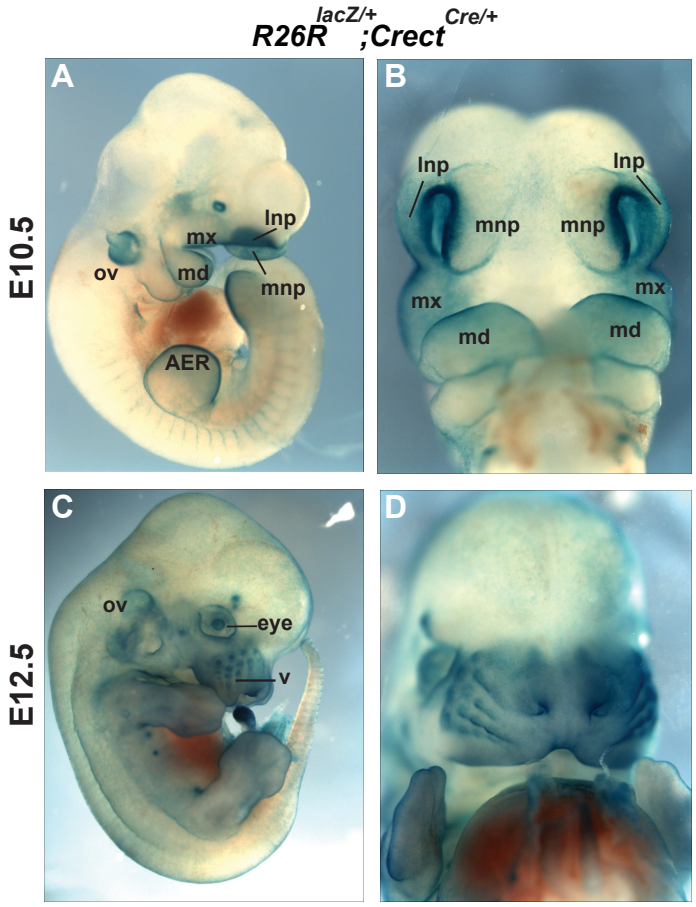

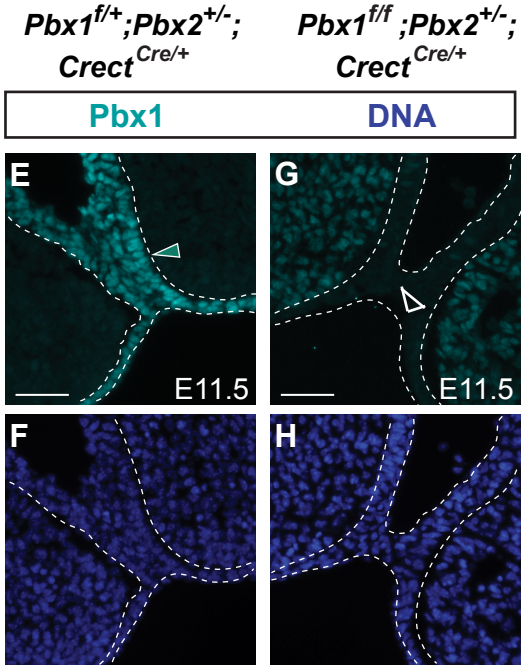

Figure S2. Crect activity in embryonic surface cephalic ectoderm (A-D). Loss of Pbx1 at the lambdoidal junction epithelium in *Pbx1/2* mutant embryo (E-H). (A-D) Whole mount *R26R*$^{LacZ/+}$;*Crect*$^{Cre/+}$ embryos stained with X-gal at E10.5 (A,B) and E12.5 (C,D). Lateral views of the whole embryo (A,C), and frontal views of the head (B,D). Crect activity in surface ectodermal epithelium, including the facial domains, is visualized by blue staining. AER, apical ectodermal ridge; lnp, lateral nasal prominence; md, mandible; mnp, medial nasal prominence; mx, maxillary prominence; Ov, otic vesicle; v, vibrissae. (E-H) Immunofluorescence with anti-Pbx1 Ab in E11.5 control (E,F) and *Pbx1/2* mutant (G,H) embryo shows complete loss of Pbx1 (aqua green) in the mutant λ junction (G). Ectodermal epithelium at the λ junction is delimited by white dashed lines. DAPI stains cell nuclei (blue; F,H). Scale bar: 100 μm.

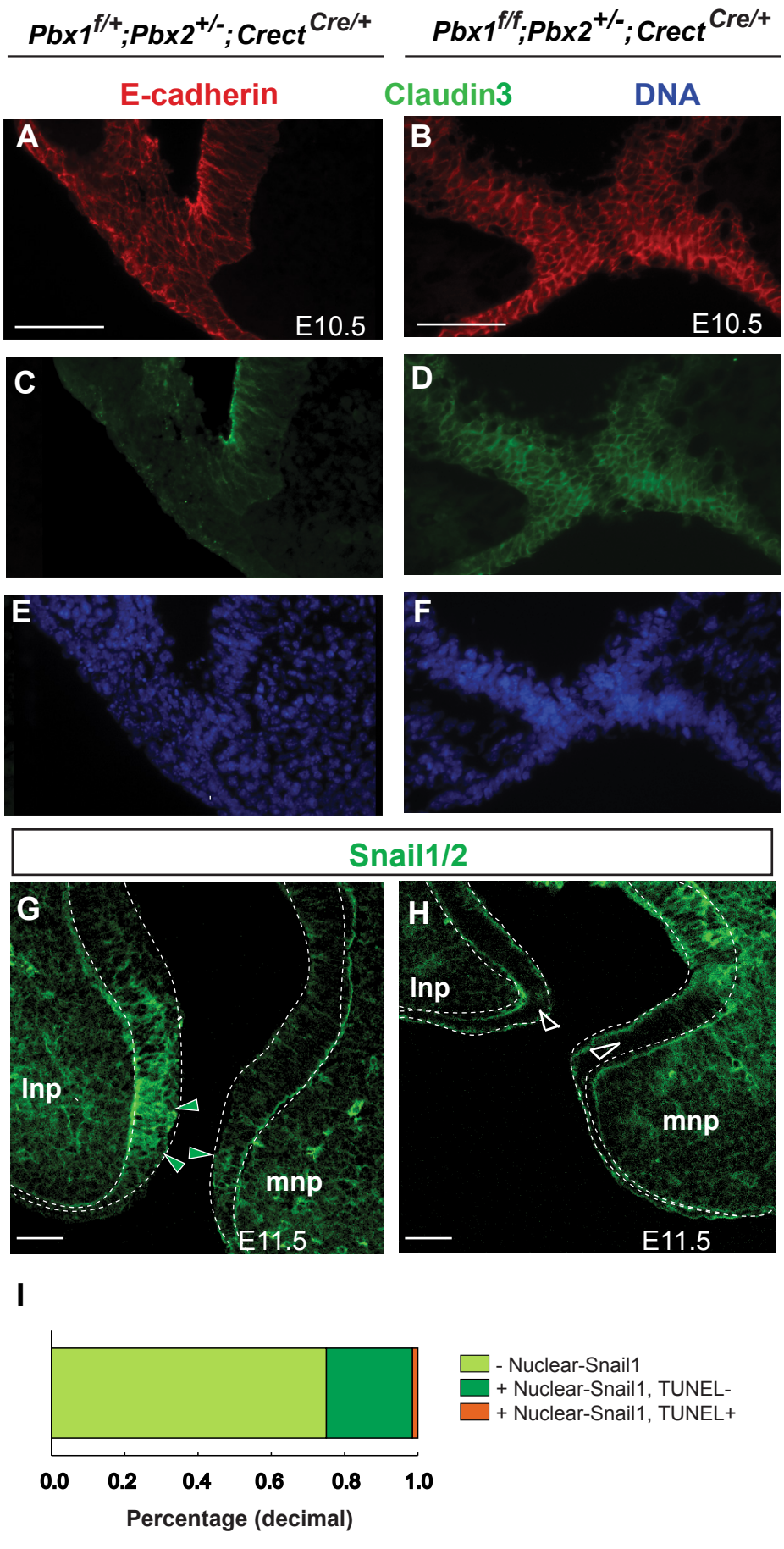

Figure S3. Pbx1 is required for the activation of EMT signatures during upper lip morphogenesis and fusion. (A-F) Double immunofluorescence labeling of E10.5 control (A,C) and *Pbx1/2* mutant (B,D) embryos for E-cadherin (red) and claudin3 (green) at the λ junction. DAPI stains cell nuclei (blue; E,F). (G,H) Immunofluorescence of Snail1 (green) at the λ junction of E11.5 control (G) and *Pbx1/2* mutant (H) embryo. Solid green arrowheads point to the presence of high levels of Snail1 protein in epithelial cells at the lnp tip; lower levels of Snail1 are also detectable in sparse epithelial cells of the apposing mnp. Empty arrowheads indicate the absence of Snail1 at the distal end of lnp and mnp in *Pbx1/2* mutant embryo. Dashed white lines define epithelial layer. Scale bars: 25μm. (I) Quantitation of immunofluorescence experiments assessing levels of Snail1 and apoptosis (via TUNEL assay) on E10.75 embryonic sections of λ junctions. Epithelial cells with nuclear Snail1 signal values above the background were approximately 25%, of which only approximately 6% were concomitantly TUNEL-positive. The latter population represents around 1.5% of all epithelial cells at the λ junction.

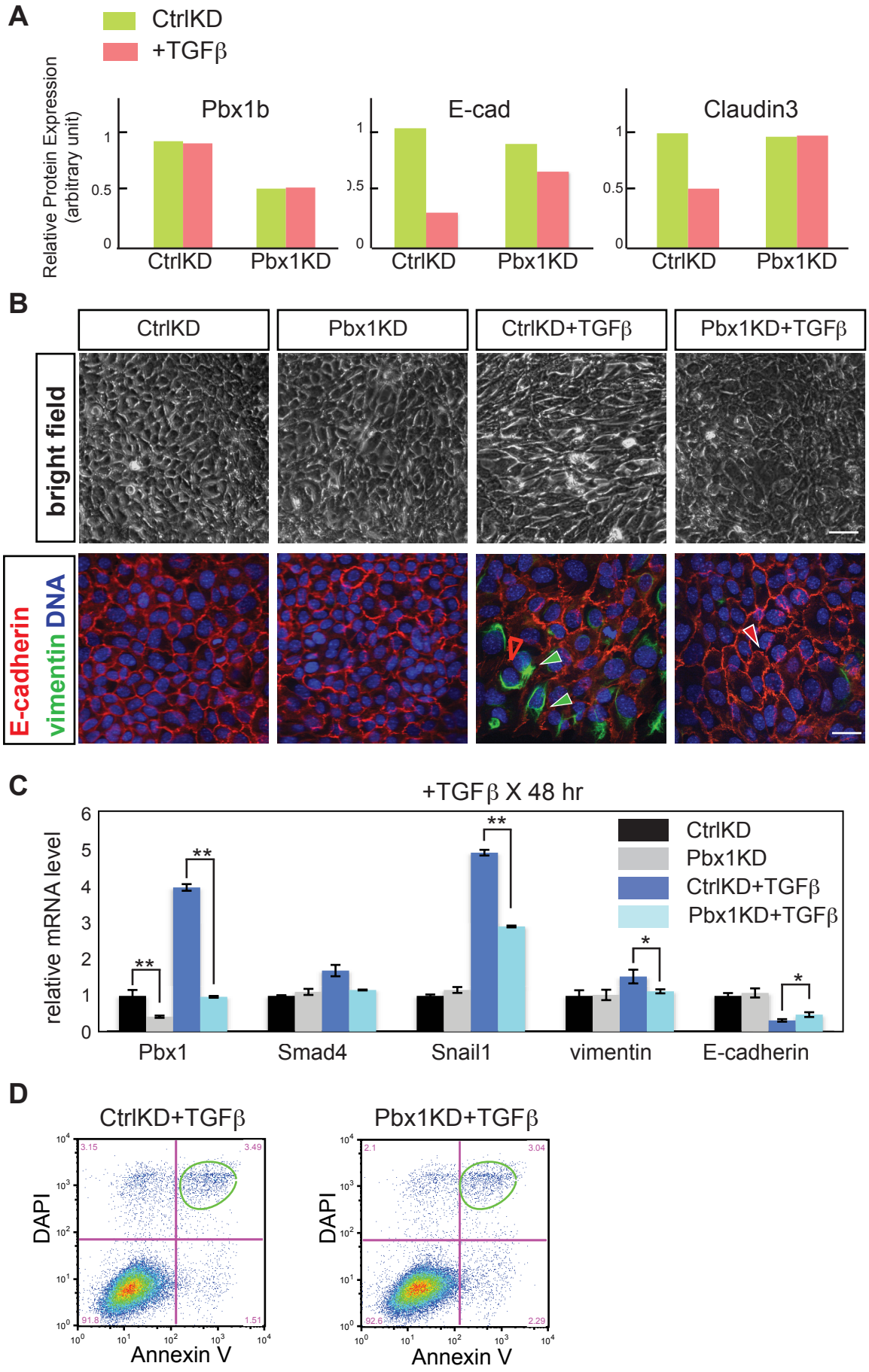

Figure S4. Quantitation of the effects of Pbx1 knockdown in NMuMG cells treated with TGFβ. (A) Quantitation of Western blot analysis shown in Figure 6N. (B) Effect of Pbx1 siRNA (Pbx1KD) on cell morphology, localization and expression of E-cadherin and vimentin in NMuMG cells in the absence or presence of low doses of TGFβ (1ng/ml) for 48h compared to control cultures (CtrlKD). Solid red arrowhead highlights persistence of membrane E-cadherin; empty red arrowhead indicates dissolution of E-cadherin at the junctions; solid green arrowheads point to accumulation of vimentin. DAPI (blue) stains cell nuclei. Scale bars: 25μm. (C) Quantitative (q) RT-PCR analysis of EMT-related gene expression in NMuMG cells cultured under condition described in (B). qRT-PCR values are normalized to the housekeeping gene TBP. Three biological replicate experiments were performed, each one in triplicate. Data are presented as Mean ± SD. * $P < 0.05$; ** $P < 0.01$ by 2-tailed Student Test. (D) Assessment of apoptosis in NMuMG cells treated with TGFβ (1ng/ml) for 48h in the presence of Pbx1 siRNA (Pbx1KD) or scrambled siRNA (CtrlKD). Cells were stained with Annexin V Alexa Fluor 488 and DAPI, followed by flow cytometric analysis. No significant differences in the percentage of late apoptotic cells (exhibiting high levels of Annexin V and DAPI staining; green circles) were observed between CtrlKD+TGFβ (3.49%) and Pbx1KD+TGFβ cells (3.04%). $P > 0.5$ (not significant).